# Shh-Proteoglycan Interactions Regulate Maturation of Olfactory Glomerular Circuitry

**Laura Persson,[1,2]* Rochelle M. Witt,[1,2†] Meghan Galligan,[1,2#] Paul L. Greer,[2] Adriana Eisner,[1,2] Maria F. Pazyra-Murphy,[1,2] Sandeep R. Datta,[2] Rosalind A. Segal[1,2]**

[1] Department of Cancer Biology, Dana-Farber Cancer Institute, Boston, Massachusetts

[2] Department of Neurobiology, Harvard Medical School, Boston, Massachusetts

*Received 23 December 2013; revised 30 April 2014; accepted 4 June 2014*

**ABSTRACT:** **The olfactory system relies on precise circuitry connecting olfactory sensory neurons (OSNs) and appropriate relay and processing neurons of the olfactory bulb (OB). In mammals, the exact correspondence between specific olfactory receptor types and individual glomeruli enables a spatially precise map of glomerular activation that corresponds to distinct odors. However, the mechanisms that govern the establishment and maintenance of the glomerular circuitry are largely unknown. Here we show that high levels of Sonic Hedgehog (Shh) signaling at multiple sites enable refinement and maintenance of olfactory glomerular circuitry. Mice expressing a mutant version of Shh ($Shh^{A1a/A1a}$), with impaired binding to proteoglycan co-receptors, exhibit disproportionately small olfactory bulbs containing fewer glomeruli. Notably, in mutant animals the correspondence between individual glomeruli and specific olfactory receptors is lost, as olfactory sensory neurons expressing different olfactory receptors converge on the same glomeruli. These deficits arise at late stages in post-natal development and continue into adulthood, indicating impaired pruning of erroneous connections within the olfactory bulb. In addition, mature $Shh^{A1a/A1a}$ mice exhibit decreased proliferation in the subventricular zone (SVZ), with particular reduction in neurogenesis of calbindin-expressing periglomerular cells. Thus, Shh interactions with proteoglycan co-receptors function at multiple locations to regulate neurogenesis and precise olfactory connectivity, thereby promoting functional neuronal circuitry.** © 2014 Wiley Periodicals, Inc. Develop Neurobiol 00: 000–000, 2014

***Keywords:*** **Shh; olfactory bulb; calbindin; proteoglycan; glomeruli; axon pruning**

## INTRODUCTION

Proper functioning of the olfactory system relies on precise connectivity that is particularly evident in the olfactory bulb glomerulus, where axons of olfactory sensory neurons (OSNs) transmit olfactory information to mitral and tufted relay neurons in an intricate information processing network. Each OSN expresses a single type of odorant receptor (OR), and within each bulb all OSNs expressing the same OR project to one of two glomeruli whose spatial positions are consistent from animal to animal, thus establishing a highly stereotyped glomerular map. Since all OSNs projecting to a single glomerulus express the same OR and respond to the same set of olfactory stimuli,

Additional Supporting Information may be found in the online version of this article.

*Correspondence to*: R. Segal (Rosalind_segal@dfci.harvard.edu).
*Present address: Stanford University
†Present address: Weill Cornell Medical Center
#Present address: Stanford University Medical School

Contract grant sponsor: The Emerald Foundation, Inc.
Contract grant sponsor: NIH Director's Pioneer Award; contract grant numbers: DP1 OD000839 (to R.A.S.), T32CA009361 (to A.E.).
Contract grant sponsor: NIDCD; contract grant number: RO1DC011558.
Contract grant sponsor: Nancy Lurie Marks Foundation (to P.L.G.) and Lefler Center.

Published online 00 Month 2014 in Wiley Online Library (wileyonlinelibrary.com).
DOI 10.1002/dneu.22202

the glomerular map is considered to represent olfactory space (Ressler et al., 1994; Vassar et al., 1994; Mombaerts, 2001).

The process of glomerular development involves an initial critical period with regulated targeting of olfactory sensory neurons (Tsai and Barnea, 2014, Ma et al., 2014), followed by a refinement period during which "unlike" axons are pruned to resolve the homogeneous mature glomeruli (Zou et al., 2004). As new OSNs continue to be generated throughout life, mechanisms must exist that allow continual glomerular modification while maintaining precise circuitry.

Glomerular circuitry also requires connections from a heterogeneous population of inhibitory olfactory interneurons situated in the glomerular layer (GL). These periglomerular (PG) interneurons modulate output signals from the glomeruli via feedforward inhibition of mitral cells, and thus facilitate odor discrimination (Aungst et al., 2003). Like OSNs, olfactory interneurons are generated throughout life. Post-natally, new interneurons originate in the Subventricular Zone (SVZ) and migrate along the Rostral Migratory Stream (RMS) to reach the OB (Alvarez-Buylla and Garcia-Verdugo, 2002; Carleton et al., 2003). This turnover of periglomerular cells provides an additional opportunity for glomerular circuit modification. Thus, glomerular circuitry involves both establishment of precise neuronal networks and continual turnover of cellular components and connections.

Despite the importance of glomerular circuitry in olfactory information processing, the mechanisms that regulate the establishment and refinement of this network are not yet understood. However, several components, including the morphogen Sonic Hedgehog (Shh), have been implicated in regulating various stages of olfactory development. Shh plays a role in the early development of OSNs and has been implicated in initial OSN axon branching and innervation of the olfactory bulb (Gong et al., 2009). At later stages, Shh promotes proliferation of olfactory interneuron progenitor populations in the SVZ and also functions as a chemoattractant, promoting the migration of neuroblasts along the RMS (Palma et al., 2005; Hor and Tang, 2010). Thus, Shh has the potential to regulate multiple, complementary cellular constituents of the glomerular circuit.

To address the role of Shh in development and maintenance of glomerular circuitry, we analyzed mice expressing a mutant version of Shh ($Shh^{Ala/Ala}$ or B6;129S4-$Shh^{tm1.1Rseg}$/J). $Shh^{Ala}$ protein binds with normal affinity to the primary Shh receptor Patched (Ptch1), but has impaired binding to specialized heparin sulfate proteoglycans containing glypican 5 and 2-*O*-sulfo-iduronic acid that function as Shh co-receptors (Witt et al., 2013). Biological responses that require high levels or prolonged duration of Shh signaling depend on proteoglycan co-receptors and are altered in $Shh^{Ala/Ala}$ mice; however, the mice are fully viable into adulthood enabling an evaluation of Shh functions throughout life (Chan et al., 2009). Here we show that mature $Shh^{Ala/Ala}$ mice exhibit disproportionately small olfactory bulbs that contain fewer glomeruli. Altered structure of the glomeruli is associated with aberrations both in interneuron neurogenesis and in olfactory sensory neuron innervation of the glomerular layer. Strikingly, mutant animals exhibit a disproportionate deficiency in neurogenesis of calbindin-expressing periglomerular cells in the SVZ. In addition, axons that express distinct olfactory receptors converge inappropriately within the olfactory bulb and so individual glomeruli include OSN axons expressing distinct olfactory receptors. Surprisingly these abnormalities in glomerular components and circuitry arise after the critical period for olfactory development (Tsai and Barnea, 2014, Ma et al., 2014) in the late post-natal period, during the period of glomerular refinement and pruning. Thus, Shh-proteoglycan signaling acts at late stages of development in multiple locations to coordinately regulate neurogenesis and the formation of precise olfactory connections, and thereby promotes establishment and maintenance of neuronal circuitry.

## MATERIALS AND METHODS

### Animals

All procedures were performed in accordance with the National Institutes of Health guidelines and were approved by the Dana-Farber Cancer Institutional Animal Care and Use Committee. Wild-type or $Shh^{Ala/Ala}$ (aka B6;129S4-$Shh^{tm1.1Rseg}$/J) (Chan et al., 2009) age-matched littermate pairs on Bl6 background were analyzed at P15 (juveniles) or 3 to 4 months of age (adult), unless otherwise indicated. M71iGFP and M72iRFP (strains B6;129P2-Olfr151$^{tm22\text{-}Mom}$/MomJ and B6;129P2-Olfr160$^{tm7Mom}$/MomJ, respectively) were obtained from Jackson Laboratories. Initially, homozygous lines of M71iGFP and M7iRFP were created by crossing mutants from each line to each other. Next, homozygous M71iGFP and M72iRFP mice were crossed with $Shh^{Ala/Ala}$ mice from our lab to generate $Shh^{Ala/+}$ mice expressing M71iGFP or M72iRFP. $Shh^{Ala/+}$ offspring expressing both RFP and GFP tagged ORs were generated, then crossed with one another to yield wild-type and $Shh^{Ala/Ala}$ littermate pairs expressing one allele of both the RFP- and GFP-tagged receptors.

## Immunohistochemistry (IHC)

Following intracardial perfusion with 4% PFA in PBS, brains were removed and post-fixed in 4% PFA in PBS before dissecting olfactory bulbs (OBs). Cryoprotected olfactory bulbs were sectioned into 12 μm slices using a Leica CM3050 cryostat and mounted on Fisher brand Superfrost Plus slides. Sections were permeabilized for 10 mins in a solution of 10% normal goat serum (NGS) and 0.1% Triton-X-100 in PBS, then blocked with 1% bovine albumin (BSA), 10% NGS, and 0.1% Triton-X-100 in PBS for 1 h at room temperature. Slides were incubated in primary antibody solution overnight at 4°C using: rabbit anti-parvalbumin (Swant) at 1:500, rabbit anti-tyrosine hydroxylase (Pel-Freez) at 1:1000, rabbit anti- calretinin (Swant) at 1:2000, rabbit anti-calbindin (Cell Signaling) at 1:200, and rabbit phospho-histone H3 (Cell Signaling) at 1:500. Secondary antibody (Invitrogen Alexa Fluor goat anti-rabbit, either 488 or 546) was used at 1:500 in block solution for 1 h at room temperature, then counterstained with 4',6-diamidino-2-phenylindole, or DAPI (5 mg/mL in $ddH_2O$), to visualize nuclei. For Calbindin staining, IHC sections underwent an additional antigen retrieval (AR) step using a 10 m*M* Sodium Citrate solution at 95°C for 15 mins, then placed in a blocking solution and stained as above. TUNEL staining of the olfactory bulb was done according to manufacturer's protocol (Promega).

## Imaging

Sections were imaged using a Nikon Eclipse Ti inverted microscope with the 10× or 20× objective (CFI Plan Fluor; N.A. 0.3, W.D. 16 mm). To produce an image of the entire half bulb, the scanning feature of NIS Elements was used to take a series of sequential images which were then stitched together using NIS Elements.

Interneuron densities were calculated using NIS Elements software to measure the areas of layers in the bulb and to count total numbers of positive cells. The exact area designations for density measurements were decided based on the localization pattern of the individual population being analyzed. Calbindin (CB) and tyrosine hydroxylase (TH) were quantified in the glomerular layer only. Parvalbumin (PV) was quantified in the glomerular and external plexiform layers. Because of high calretinin (CR) density, calretinin positive cells were quantified only in a portion of the bulb, designated by finding the middle 600 μm along the dorsal-ventral axis and counting within these bounds in all layers. Total interneuron counts were divided by area measurements to produce final densities of cells/$\mu m^2$. Between 10 and 16 half bulbs were analyzed per animal for each interneuron subtype.

To assess mitral cell number, the DAPI-labeled cells located in the mitral layer were counted in eight olfactory bulb sections from 3 mutants and three wild-type adults. Granular layer area was calculated by measuring the total granular area divided by the total olfactory bulb area in eight sections from thre animals per genotype. The number of TUNEL positive cells in the glomerular layer was assessed in X sections in three animals per genotype. The number of phospho-Histone H3 stained cells in the dorsal or ventral half of the SVZ was determined on eight matched coronal sections from three adult animals per genotype.

For Shh staining sections were incubated for antigen retrieval in 1 m*M* EDTA, 10 m*M* Tris pH 8 at 95°C for 10 mins and then cooled at room temperature for 30 mins. Slides were then washed and stained with primary antibody (Abcam Shh anti-rabbit) diluted 1:100.

For imaging of M71 and M72 lines, glomerular imaging was done on either a Nikon Eclipse Ti inverted microscope or a Nikon Eclipse E800 upright microscope using the 10× or 20× objective (CFI Plan Fluor 20×; N.A. 0.5, W.D. 2.1 mm). Multichannel images were collected using a Coolsnap HQ 12-bit monochrome CCD camera for fluorescence imaging.

## EdU Labeling

For adult mice, 5-ethynyl-2'-deoxyuridine (EdU) was administered by intraperitoneal (IP) injection to age-matched littermate pairs at a concentration of 50 mg EdU/kg body weight. Adults received a total of four EdU injections, once per week, starting at 3 months of age. Subjects were sacrificed at 4 months of age and intracardially perfused as above.

For juvenile mice, pregnant mothers received a single IP injection of EdU (50 mg/kg body weight) at day E14.5 of pregnancy. Age-matched littermate pups received two subsequent EdU injections (of same concentration) at postnatal days 5 and 11 and were sacrificed by isoflurane inhalation at postnatal day 15.

For costain experiment, EdU staining was begun immediately following completion of the interneuron secondary antibody incubation. Sections were permeabilized for 20 mins in 0.5% Triton X-100 in PBS at room temperature. After washing, they were incubated with EdU reaction mixture (4.3 mL 1X Click-iT reaction buffer, 200 μL $CuSO_4$, 12.5 μL Alexa Fluor azide, and 500 μL reaction buffer additive in 5 mL) for 30 mins at room temperature in a dark chamber. Sections were then washed and counterstained with DAPI as described above.

EdU-positive cells were demarcated and then examined for overlap with interneuron markers. For every half bulb, both the total number of EdU-positive cells and the number of EdU-positive cells that colocalized with a given interneuron marker were recorded. The number of co-positives was normalized to the total number of EdU-positive cells to yield a fraction representing the percentage of EdU-positive cells that are co-positives. Analysis was done by a researcher blinded to genotype.

Quantification in juveniles was performed as above or using an automated counting script run in the Fiji version of ImageJ. Quantification of TH and CR was performed manually and was restricted to the glomerular layer, or the middle third of the glomerular layer along the dorsal-ventral axis, respectively. Within the designated areas, total numbers of EdU positive cells were counted by an individual

blinded to genotype, followed by numbers of cells considered to be co-positive for EdU and an interneuron marker. Final values were calculated as fractions of EdU positive cells co-positive for a given marker in individual bulb images.

Automated counting was performed for CB and PV stained sections using a program written for Fiji in collaboration with the Neuroimaging Core at Harvard Medical School. The program output included both total EdU counts and co-positive counts for the glomerular layer in the case of CB and for the GL and EPL together in the case of PV. A total of 10 to 16 half bulbs were analyzed per animal per interneuron subtype.

## mRNA and qPCR

The entire olfactory epithelium from either wild type or $Shh^{(ala/ala)}$ mice was dissected and homogenized in 1 ml Trizol (Invitrogen). RNA was isolated following the manufacturer's instructions, and the purified nucleic acid was resuspended in 200 μL XB buffer (picopure kit, Arcturus). Contaminating genomic DNA was removed by RNAse-free DNAse digestion (Qiagen) and column purified using the picopure kit according to the manufacturer's instructions. The purified RNA was quantified by nanodrop, and 1 μg of total RNA per mouse was converted to cDNA by reverse transcription with SuperscriptIII (Invitrogen) per manufacturer's instructions. qRT-PCR was performed using Power SYBR green master mix, and all reactions were performed in triplicate. The expression of olfactory receptors was normalized to the expression of gapdh. Probes used were: *Shh* (Mm00436527_m1), *Ptch1* (Mm00436026_m1), *Glypican 5* (Mm00615599_m1), *Gli1* (Mm00494645_m1), *MOR23* (F: TGCTCACAGCAATGGGTTATGATCGTT, R: TGGC TGGCACATGAAGAACTGCC), *MOR28* (F: TCGCTATG TGGCCATTTGTAAACCTT, R: AGATATGGAGTGTATG GTCCCTGCTG), *M72* (F: TGCCATGGGACTCATAGGC TCAA, R: AGCAAGAGAGCTTCATGAGGGGG), *174-9* (F: AGTCAGCAAGTGGACGCCGC, R: ACACAGAGGCC ACTTTTACGGTATGC), *P2* (F: ACCATTCCTTCCTTGG CTGTGC, R: TGCAAGGGATCACAGATCGCCA).

## Glomerular Morphometry

Sections for morphometric study were chosen from adult animals (3–4 months of age) at various points along the olfactory bulb (20%, 35%, 50%, 65%, and 80% positions). Images were edited using Adobe Photoshop and analyzed using MetaMorph Offline (Meta Imaging Series). Each section was analyzed for glomerular number. Glomerular size was assessed by measuring the area of individual glomeruli.

For analysis of juvenile animals, coronal sections for analysis were chosen from M71-GFP M72-RFP animals at P15 based on the first emergence of the lateral RFP glomerulus in each olfactory bulb. Within this section the area of each glomerulus was found using the area measurement tool in NIS Elements and the total number of glomeruli per section was counted. Four wild-type/mutant pairs were analyzed. Researcher was blind to genotype.

## NCAM, OMP Immunohistochemistry, and *In Situ* Hybridization

For immunohistochemistry with NCAM antibodies (rat; Chemicon) or OMP antibodies (rabbit; Abcam) sections were treated with antigen retrieval solution (0.5% 1 *M* Tris buffer [pH 8.0] and 0.2% 0.5 *M* EDTA in PBS) for 15 mins at 95°C. Following a 30 min cool-down period at room temperature, sections were washed, permeabilized, and immmunostained overnight at 4°C in primary antibodies (αOMP, 1:250; αNCAM, 1:1000). Secondary antibodies were Alexa 488- or Alexa 546-conjugated (Molecular Probes, 1:500). All sections were stained with DAPI, washed in PBS, and mounted as previously described. *In situ* hybridization performed as previously described (Chan et al. 2009).

# RESULTS

## $Shh^{Ala/Ala}$ Mice Exhibit Altered Glomerular Morphology

While overall brain size is reduced in $Shh^{Ala/Ala}$ mice, the cerebellum and the olfactory bulbs (OBs) are disproportionately small; adult $Shh^{Ala/Ala}$ animals exhibit a 30% reduction in olfactory bulb volume compared with wild-type littermates [Fig. 1(A)] (Chan et al., 2009). Given the highly stereotyped nature of the olfactory glomerular map, a reduction in size of the OB might perturb glomerular structure or number. We observe a 30% reduction in the number of glomeruli in $Shh^{Ala/Ala}$ olfactory bulbs compared with wild-type; this reduction is seen throughout the bulb [Fig. 1(B)]. In contrast, the mean size of individual glomeruli (glomerular area) is unchanged. The magnitude of the granular zone is also not significantly altered in $Shh^{Ala/Ala}$ mice [Fig. 1(C), Supporting Information Fig. 1(A)], nor are differences observed in mitral cell number [Supporting Information Fig. 1(B)]. These findings implicate Shh as a novel regulator of glomerular number.

Several potential changes in circuitry might accompany altered glomerular number in $Shh^{Ala/Ala}$ olfactory bulbs. As there are fewer glomeruli, it is possible that there is aberrant innervation of the glomerular layer by OSNs. In this scenario, OSNs might innervate interglomerular spaces, incorrect glomerular targets, or both. We examined Neural Cell Adhesion Molecule (NCAM) and Olfactory Marker Protein (OMP) immunostaining on olfactory bulb coronal sections to visualize OSN axons in the glomerular layer, and found that OSNs correctly innervate the glomeruli without aberrant targeting to interglomerular spaces [Fig. 2(A,B)]. We then examined the possibility of an abnormality in the distribution of OSNs to their appropriate glomeruli. Specifically, fewer glomeruli could result from a

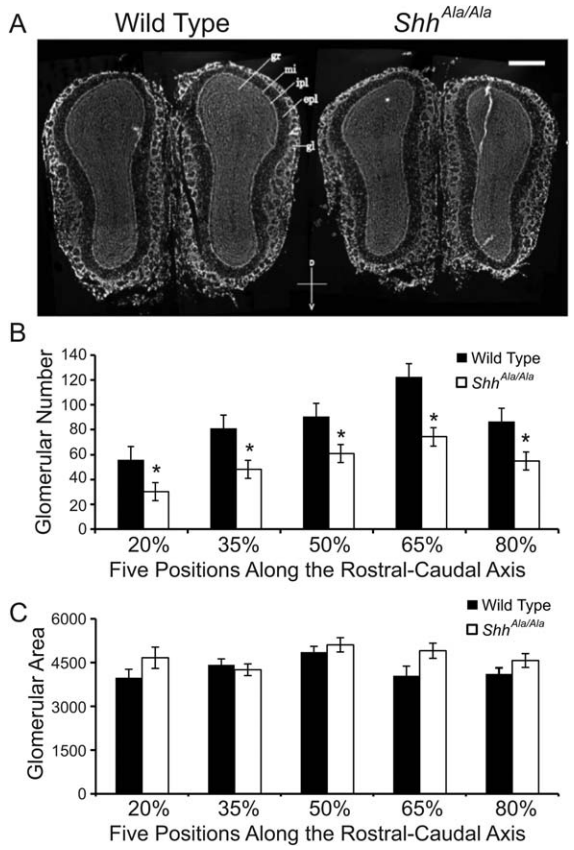


**Figure 1** *Shh*$^{Ala/Ala}$ mice have smaller olfactory bulbs (OBs) with fewer glomeruli. (A) Coronal sections from wild-type (right) and *Shh*$^{Ala/Ala}$ (left) OBs at the midpoint along the rostral-caudal axis. Scale bar = 500 μm. gl = glomerular layer, epl = external plexiform layer, ipl = internal plexiform layer, mi = mitral cell layer and gr = granular layer. (B) Average glomerular number for wild-type and *Shh*$^{Ala/Ala}$ mice at distinct positions along the rostral-caudal axis. Error bars = SEM, N = 3 pairs of mice, $*p < 0.05$ by student's *t*-test with Bonferroni correction. (C) Average glomerular area for wild-type and *Shh*$^{Ala/Ala}$ mice at distinct positions along the rostral-caudal axis. Error bars = SEM, $N = 3$ pairs of mice.

"mixing" of OSNs expressing distinct receptors within single glomeruli [Supporting Information Fig. 2(A)]. To test this idea we examined transgenic mice expressing GFP and RFP under the control of the M71 and M72 OR promoters respectively (strains B6;129P2-*Olfr151*$^{tm22Mom}$/MomJ and B6;129P2-*Olfr160*$^{tm7Mom}$/MomJ, respectively). We crossed the M71-GFP/M72-RFP animals to the *Shh*$^{Ala/Ala}$ mice. Normally, M71 and M72 axons project to two sets of neighboring glomeruli. A comparison of the wild-type and *Shh*$^{Ala/Ala}$ littermates expressing RFP and GFP demonstrated mixing between RFP- and GFP-expressing axons in at least one glomerulus in most *Shh*$^{Ala/Ala}$ mice (three out of five examined). This phenotype is not seen in adult wild-type animals [Fig. 2(D)]. There are two sets of M71 and M72 glomeruli in each bulb, one lateral and one medial pair; axon mixing was seen only in the lateral glomerular pair [Fig. 2(C)] (Potter et al., 2001). The mixing of OSNs expressing distinct receptors could account for the reduction in the number of glomeruli seen in *Shh*$^{Ala/Ala}$ mice, and implicates Shh signaling in the process of developing "pure" glomeruli. Studies addressing the alternative that *Shh*$^{Ala/Ala}$ mice express fewer distinct receptors, thereby necessitating fewer individual glomeruli, did not demonstrate any change in receptor expression [Supporting Information Fig. 2(B)].

## Generation of Calbindin Positive Periglomerular Interneurons is Reduced in *Shh*$^{Ala/Ala}$ Mice

In addition to the highly specific organization of OSN inputs, glomerular circuitry depends on appropriate connections formed by inhibitory interneurons. Distinct interneuron subpopulations can be identified by expression of four neurochemical markers: tyrosine hydroxylase (TH), parvalbumin (PV), calretinin (CR), or calbindin (CB). These markers define non-overlapping cell populations and collectively account for the majority of olfactory interneurons in adult mice (Batista-Brito et al., 2008; Lledo et al., 2008). Adult *Shh*$^{Ala/Ala}$ mice (3–4 months of age) have a dramatic 35% reduction in the density of CB-expressing interneurons, while no changes are found in the densities of TH, PV, or CR expressing populations [Fig. 3(A–E)]. A density analysis was used to account for the reduced size of the adult olfactory bulb in *Shh*$^{Ala/Ala}$ mice, thereby highlighting only disproportionate reductions of interneuron number. To rule out the possibility that expression of the CB protein itself is pervasively altered in the mutant animals, we examined a population of CB-expressing interneurons in M1 cortex, which originate from a distinct progenitor region (Fogarty et al., 2007). The density of CB-expressing cells in this region did not differ in wild-type and *Shh*$^{Ala/Ala}$ mice, indicating that the reduction in CB+ cells in the olfactory bulb does not simply reflect a global loss of marker expression in these mice [Fig. 3(F,G)].

Because Shh has well-known roles as a mitogen required for generating olfactory interneurons, we analyzed production of these four distinct olfactory interneuron populations. We used EdU injections and labeling to identify neurons born between 3 and 4 months of age, and compared density of EdU-positive cells in the olfactory bulbs of wild-type and *Shh*$^{Ala/Ala}$ littermates [Fig. 4(A)]. There is a dramatic,

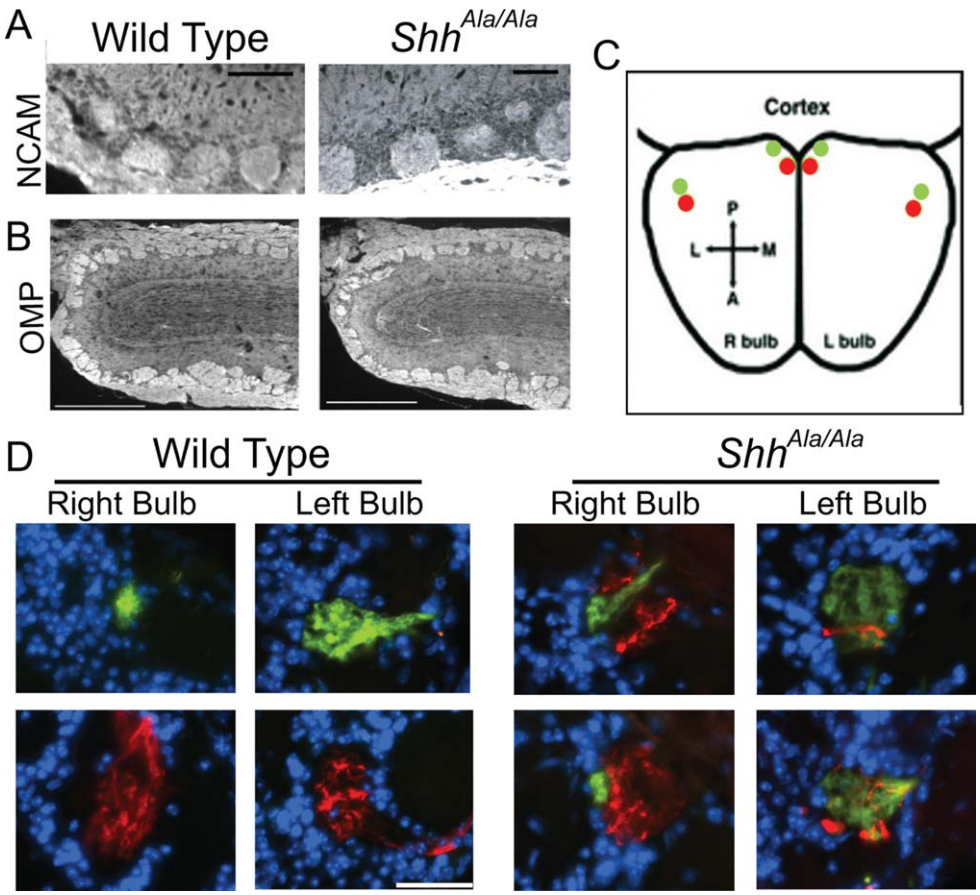


**Figure 2** *Shh*$^{Ala/Ala}$ mice show aberrant co-innervation of M71 and M72 OSN axons within single glomeruli. (A) NCAM and (B) OMP immunostaining in the glomerular layer to visualize incoming OSN axons. No staining visible in interglomerular spaces in either wild-type or *Shh*$^{Ala/Ala}$ mice. Scale bars = 100μm in A and 1000 μm in B. (C) Diagram of the dorsal surface of the mouse main olfactory bulbs showing the locations of the medial and lateral M71 and M72 glomerular pairs in green and red, respectively. (D) GFP and RFP expressing M71 and M72 axons, respectively, innervating the glomerular layer in wild-type and *Shh*$^{Ala/Ala}$ mice. Glomeruli shown are from the lateral pair in both left and right OBs. Scale bar = 50 μm.

40% reduction in the density of new neurons overall in the olfactory bulbs of *Shh*$^{Ala/Ala}$ mice compared with wild-type littermates [Fig. 4(B)]. Strikingly, this reflects a disproportionate reduction in new production of calbindin-expressing interneurons; *Shh*$^{Ala/Ala}$ mice show a 75% reduction in the percentage of EdU+ cells co-labeled with calbindin compared with wild-type littermates. In contrast, the proportion of EdU+ cells co-labeled with TH, PV, and CR is not significantly different between wild-type and *Shh*$^{Ala/Ala}$ mice [Fig. 4(C–G)]. Levels of apoptosis in the olfactory bulb are unchanged in *Shh*$^{Ala/Ala}$ mice (Supporting Information Fig. 3) Olfactory interneurons are generated in the SVZ, and proliferation in the SVZ is reduced in adult *Shh*$^{Ala/Ala}$ mice [Fig. 4(H); Chan et al., 2009)]. Thus, Shh signaling has a specific role in adult neurogenesis of olfactory calbindin-positive interneurons and this results in a perturbation of the interneuron composition of the glomerular layer in adult *Shh*$^{Ala/Ala}$ mice. Combined with the observed defects in OSN innervation of the glomerular layer, these data demonstrate that Shh regulates glomerular circuitry by affecting both cellular components and precise wiring of the olfactory glomeruli.

## Juvenile *Shh*$^{Ala/Ala}$ Mice Display no Change in Glomerular Structure or Innervation

We next sought to define a developmental timeframe for these effects. We analyzed P15 *Shh*$^{Ala/Ala}$ mice for changes in glomerular morphology, OSN targeting to M71 and M72 glomeruli, density of new

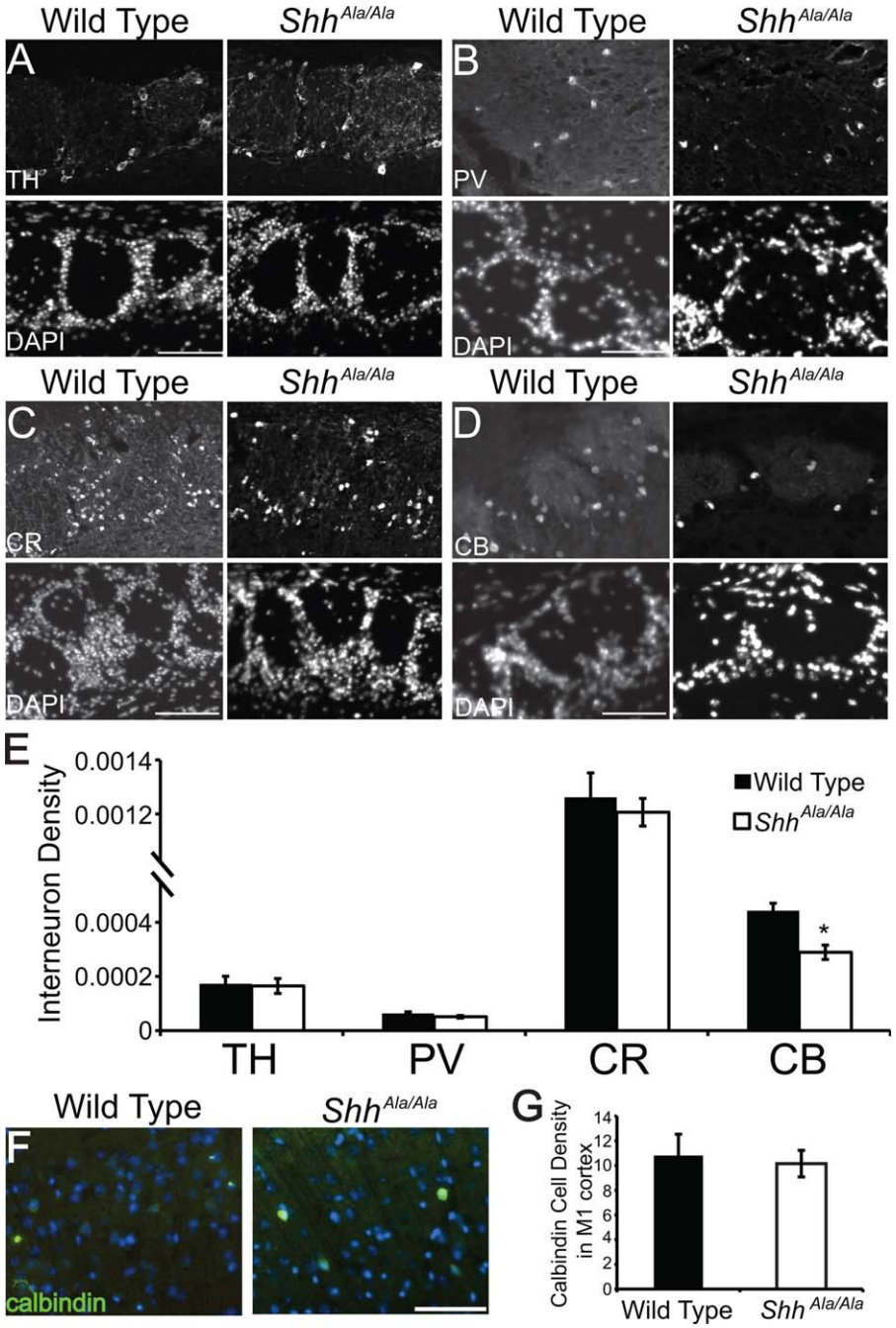


**Figure 3** *Shh*$^{Ala/Ala}$ mice show a disproportionate reduction in calbindin-expressing periglomerular cells. (A–D) Immunostaining for tyrosine hydroxylase (TH), parvalbumin (PV), calretinin (CR) and calbindin (CB) positive interneurons in the glomerular layer of 3-month-old mice. The left and right panels for each interneuron subtype are from wild-type and *Shh*$^{Ala/Ala}$ mice, respectively. DAPI was used to visualize corresponding nuclei. Scale bar = 100 μm, $N = 3–5$. (E) Average interneuron density in the glomerular layer of wild-type and *Shh*$^{Ala/Ala}$ mice by interneuron subtype. $*p < 0.05$ by student's *t*-test with Bonferroni correction. (F) Calbindin-expressing cells in M1 motor cortex of wild-type and *Shh*$^{Ala/Ala}$ mice. Calbindin shown in green and DAPI in blue. Scale bar = 100 μm. (G) Quantification of calbindin cell density in the M1 motor cortex reveals no difference between wild-type and *Shh*$^{Ala/Ala}$ mice.

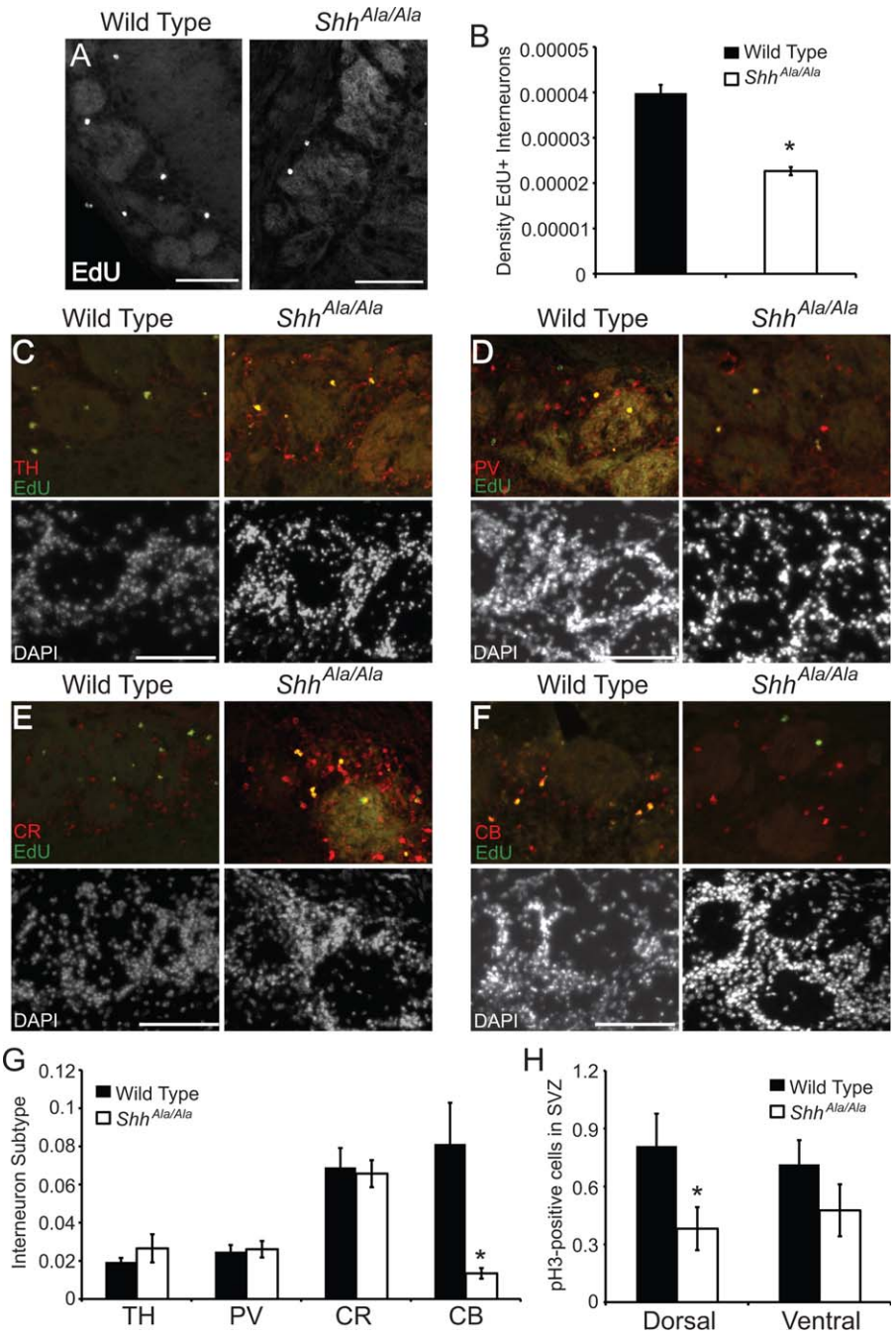


**Figure 4** Adult neurogenesis of calbindin-expressing periglomerular cells reduced in $Shh^{Ala/Ala}$ mice. (A) EdU staining in the glomerular layer of wild-type and $Shh^{Ala/Ala}$ mice at 4 months of age. Scale bar = 100 μm. (B) Quantification of EdU-positive cell density in wild-type and $Shh^{Ala/Ala}$ adult olfactory bulbs. Error bars = SEM, $N = 3$, $*p < 0.001$ by student's $t$-test. (C–F) Co-staining for EdU and tyrosine hydroxylase (TH), parvalbumin (PV), calretinin (CR), and calbindin (CB). The left and right panels for each interneuron subtype are from wild-type and $Shh^{Ala/Ala}$ animals, respectively. Interneurons shown in red, EdU in green, and DAPI in blue. Scale bar = 100 μm. (G) Subtype specific quantification of interneurons born between 3 and 4 months of age in wild-type and $Shh^{Ala/Ala}$ mice. Error bars = SEM, $N = 3$, $*p < 0.001$ by student's $t$-test with Bonferroni correction. (H) Quantification of phosphohistone H3-positive cells in the SVZ of wild-type and $Shh^{Ala/Ala}$ mice. Error bars = SEM, $*p < 0.05$ by student's $t$-test.

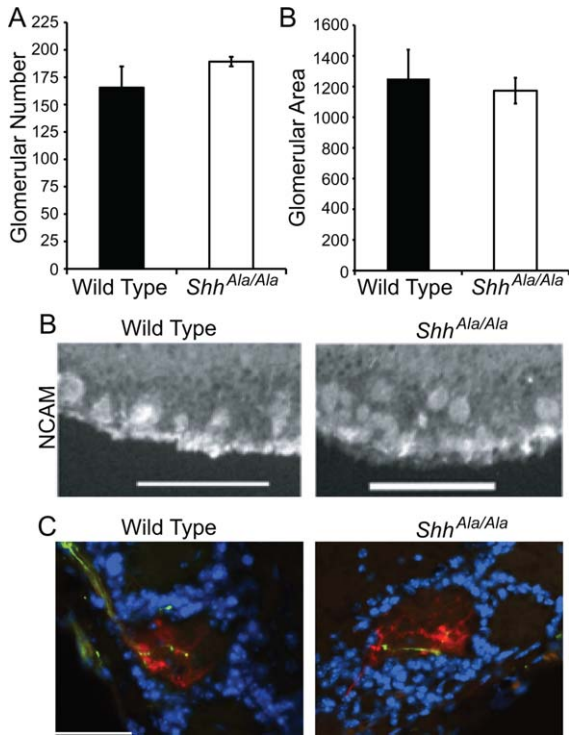


**Figure 5** Glomerular number or size, and M71 and M72-innervation are not altered in juvenile $Shh^{Ala/Ala}$ mice. (A) Average glomerular number and (B) area at the location of the lateral M72 glomeruli in wild-type and $Shh^{Ala/Ala}$ P15 mice. Error bars = SEM. (B) NCAM staining to visualize incoming OSNs to the glomerular layer. Scale bar = 500 μm. (C) M72 lateral glomeruli in wild-type and $Shh^{Ala/Ala}$ mice showing co-innervation by M71 and M72 OSNs. Scale bar = 50 μm.

neurons in the glomerular layer, and subtype specific interneuron neurogenesis. Surprisingly at P15 there are no significant differences apparent in glomerular number or size nor is there any detectable difference in granular area suggesting that Shh impacts glomerular morphology at later developmental stages [Fig. 5(A), Supporting Information Fig. 4]. As expected, NCAM staining shows no aberrant targeting of OSNs to interglomerular spaces [Fig. 5(B)]. When we analyzed axon targeting in the M71 and M72 glomeruli, we observe mixing between the axons of M71 and M72 OSNs in both wild-type and $Shh^{Ala/Ala}$ mice at this age, corroborating previous data (Zou et al., 2004). There is no apparent difference between juvenile wild-type and $Shh^{Ala/Ala}$ littermates in the quality or quantity of axonal mixing. In four pairs analyzed, three wild-type and two $Shh^{Ala/Ala}$ mice showed mixing in the lateral glomeruli, although none showed mixing in the medial glomeruli. Thus, both wild-type and $Shh^{Ala/Ala}$ juvenile phenotypes resemble the mutant adult phenotype [Fig. 5(C)]. Together these data are consistent with a role for Shh-proteoglycan signaling in the process of glomerular refinement rather than in the process of initial axon targeting and glomerular establishment.

We next examined neurogenesis in wild-type and $Shh^{Ala/Ala}$ littermates between E14.5 and P15 using EdU injections and labeling. In contrast to adult animals, no differences were observed in the density of newborn cells in the glomerular layer of juvenile $Shh^{Ala/Ala}$ mice compared with wild-type [Fig. 6(A,B)]. Furthermore, analysis of the interneuron subpopulations showed no significant differences in subtype-specific neurogenesis [Fig. 6(C)]. Most notably, proliferation of calbindin-expressing interneurons in $Shh^{Ala/Ala}$ mice is unaltered at this age. Thus, the observed defects in $Shh^{Ala/Ala}$ adult mice appear to be the result of altered signaling during later developmental stages and adulthood. These data identify specific roles for Shh-proteoglycan interactions in the SVZ and OB during postnatal refinement and maintenance of glomerular circuitry, a process that must occur with high fidelity throughout life to maintain the precise connectivity of the olfactory system.

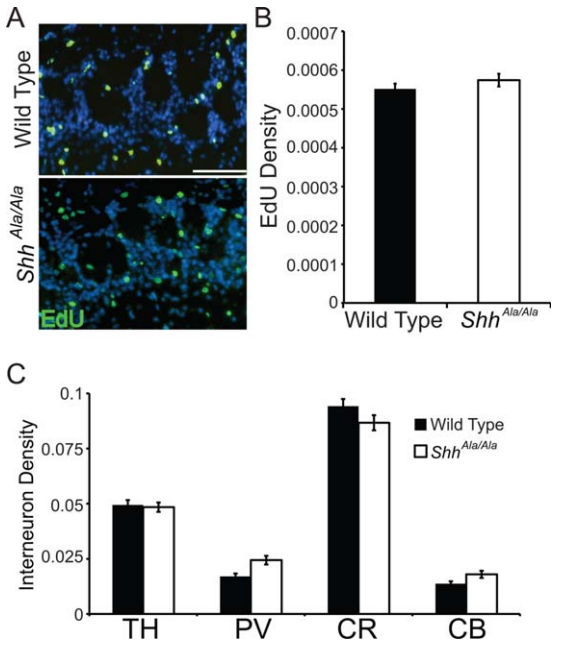


**Figure 6** Juvenile production of TH, PV, CR, and CB-expressing olfactory interneurons is unaltered in $Shh^{Ala/Ala}$ mice. (A) EdU+ cells in the glomerular layer of wild-type and $Shh^{Ala/Ala}$ P15 olfactory bulbs. EdU shown in green and DAPI in blue. Scale bar = 100 μm. (B) Quantification of EdU+ cells in both wild-type and $Shh^{Ala/Ala}$ mice. Error bars = SEM. (C) Subtype specific quantification of juvenile interneuron production in wild-type and $Shh^{Ala/Ala}$ mice. Error bars = SEM.

## Shh Signaling Within the Olfactory Bulb

The deficiency in neurogenesis of calbindin-positive interneurons reflects decreased proliferation within the SVZ, as $Shh^{Ala/Ala}$ mice exhibit reduced proliferation in this zone [Fig. 4(H); Chan et al., 2009]. To determine whether Shh has additional signaling functions within the olfactory bulb itself we examined expression of Shh in the OB both during development and in adulthood. *Shh* mRNA and protein are present both in early post-natal and adult olfactory bulbs. Shh is expressed by mitral cells within the bulb, and Shh protein can be detected in mitral cell dendrites within the glomeruli. In addition, Shh protein is detected in the periglomerular, inhibitory cells [Fig. 7(A)]. Thus, Shh has the potential to act locally within the bulb to affect glomerular formation and refinement.

To determine whether there is a deficit in Shh signaling within the olfactory bulb of $Shh^{Ala/Ala}$ mice, we examined expression of *Gli1* mRNA, a readout for pathway activity. There is no reduction in *Gli1* at P0. However, by P15 *Gli1* expression in $Shh^{Ala/Ala}$ mice is reduced to approximately 25% of the expression levels found in wild-type mice, and decreased levels of *Gli1* expression continue into adulthood [Fig. 7(B,C)]. This time course is consistent with the developmental stage when aberrant axon targeting of OSNs becomes evident in the mutant animals, and suggests that deficits in olfactory circuitry in the $Shh^{Ala/Ala}$ animals are due to altered Shh pathway activity in the olfactory bulb itself as well as in the SVZ.

Glypican 5 (GPC5) a component of the Shh co-receptor proteoglycan (Witt et al., 2013) is expressed by mitral and periglomerular interneurons, indicating the potential for active Shh-proteoglycan signaling within these cell types [Fig. 7(D)]. Furthermore, *Gli1* mRNA is also highly expressed in mitral cells and in periglomerular interneurons [Fig. 7(C)], indicating that these cells are regulated by Shh. Thus, Shh functions in the SVZ to regulate proliferation of calbindin-positive interneurons, and also acts within the bulb to affect mitral and periglomerular cells whose dendrites innervate the glomeruli. Together these findings illustrate specific roles for Shh-proteoglycan interactions in both the SVZ and the olfactory bulb during late stages of olfactory circuitry development and maintenance.

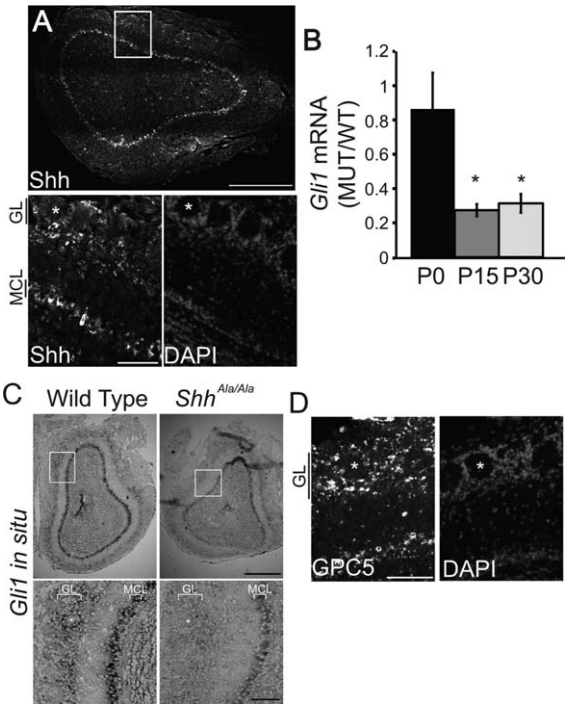


**Figure 7** Mitral cells and periglomerular interneurons in the juvenile olfactory bulb produce and respond to Shh. (A) Shh immunostaining on coronal wild-type olfactory bulb sections at P15. Whole bulb (top panel, scale bar = 500 μm) and zoomed inset of the mitral cell layer (MCL) and glomerular layer (GL) showing Shh protein (left bottom, scale bar = 100 μm) and corresponding DAPI (right bottom). Asterisks (*) are placed in middle of glomeruli. Shh protein is seen mainly in mitral cells and periglomerular interneurons. (B) *Gli1* expression in $Shh^{Ala/Ala}$ olfactory bulbs compared with wild-type at P0, P15, and P30. Vertical axis is the ratio of mutant to wild-type *Gli1*. Error bars = SEM, $*p < 0.001$ by *z*-test. (C) *Gli1 in situ* on P15 coronal sections from wild-type and $Shh^{Ala/Ala}$ mice. *Gli1 mRNA* is seen primarily in mitral cells (MCL) and periglomerular interneurons (GL) in wild-type and $Shh^{Ala/Ala}$ mice. Scale bars = 500 μm. (D) Glypican 5 (GPC5) immunostaining in wild-type P15 coronal olfactory bulb sections. Left panel is GPC5 and right panel is corresponding DAPI. Staining is seen primarily in mitral cells and periglomerular interneurons (GL). Scale bar = 100 μm.

## DISCUSSION

In this study we demonstrate that Shh signaling is critical for establishing and maintaining precise olfactory glomerular circuitry. We show that mutations that impair Shh binding to proteoglycan co-receptors and thereby diminish Shh signaling decrease proliferation of calbindin-positive olfactory interneurons. Furthermore, we reveal that diminishing Shh signaling by disrupting Shh-proteoglycan interactions results in alterations in glomerular number and heterogeneous innervation of individual glomeruli in the adult olfactory bulb. Taken together, our findings indicate that high levels of Shh signaling regulate the neuronal architecture of olfactory

glomeruli and maintain precise circuitry as olfactory neurons are replaced throughout life.

## Selective Role of Shh in Calbindin Neurogenesis

Previous studies demonstrated that Shh promotes the birth of interneurons of the olfactory bulb (Ihrie et al., 2011). However, the specificity of the neurogenesis defect observed in $Shh^{Ala/Ala}$ mice is surprising and indicates that Shh acts differentially across distinct progenitor zones of the SVZ. Shh is produced by neurons of the ventral forebrain, including those within the stria terminalis directly adjacent to the ventral SVZ, while CB-expressing interneurons originate from the most ventral regions of the SVZ, in close proximity to the Shh source (Lledo et al., 2008; Ihrie et al., 2011). Thus proliferating progenitors of CB-expressing interneurons ordinarily experience the highest possible level of Shh signaling within the SVZ. While proliferation in the dorsal portion of the SVZ is also reduced in adult $Shh^{Ala/Ala}$ mice, we postulate that a partial reduction in Shh signaling in the SVZ due to impaired proteoglycan interactions particularly affects this "highest demand" population, and so results in a disproportionate deficiency of calbindin-positive cells. Together these data suggest a model wherein different progenitor populations in the SVZ may differentially express proteoglycan receptors, or may require varying levels or durations of Shh signaling to stimulate proliferation and differentiation. This model is analogous to the mechanisms by which discrete levels of Shh signaling result in divergent cell fate choices in the developing spinal cord (Yu et al., 2013), or regulate balanced expansion of two progenitor pools during limb development (Zhulyn et al., 2014).

We considered an alternative possibility that a reduction in calbindin-positive interneurons in $Shh^{Ala/Ala}$ mice could reflect abnormalities in neuroblast migration along the rostral migratory stream to the olfactory bulb. Angot et al. found that ectopic expression of Shh could function as a chemo-attractive agent to divert migrating neuroblasts away from the rostral migratory stream (Angot et al., 2008). However, a deficit in migration cannot fully explain the disproportionate decrease in calbindin-expressing interneurons or account for reduced numbers of newborn neurons in the SVZ (Chan et al., 2009).

The extent of apoptosis in the olfactory bulb as assessed by TUNEL staining was the same in wild-type and $Shh^{Ala/Ala}$ mice, indicating that our results also cannot be explained by Shh-dependent survival of olfactory interneurons. The reduced production of CB+ interneurons in adulthood could reflect an effect of Shh signaling on fate specification of progenitors in the SVZ. Indeed, Ihrie et al. have shown that ectopic expression of Shh in the dorsal SVZ can re-specify neural stem cells to CB-expressing periglomerular cells and deep granule cells (Ihrie et al., 2011). However, respecification of CB+ progenitors in adulthood would be expected to produce a concomitant decrease in other adult-born populations and does not account for the observed deficits in SVZ neurogenesis. Thus, the data are most consistent with the explanation that a reduction in Shh signaling causes a disproportionate defect in neurogenesis of calbindin-positive cells within the SVZ and a resultant deficit in calbindin-expressing olfactory interneurons in the bulb.

Olfactory interneurons turn over throughout life. Therefore, a deficit in CB-positive periglomerular cells in $Shh^{Ala/Ala}$ mice would be expected to worsen with aging as CB-positive cells die and fail to be replaced. Overall reduction in adult olfactory bulb neurogenesis lessens inhibitory inputs that normally modulate mitral cell neurotransmission (Breton-Provencher et al., 2009). Furthermore, reduced adult neurogenesis impairs olfactory function and the ability to distinguish distinct odors (Akers et al., 2010). The effects of a specific reduction in olfactory calbindin-positive interneurons produced in adulthood are not known. However, olfactory interneurons exhibit distinctive functions based on neuronal subtype. The parvalbumin-expressing olfactory interneurons modulate mitral cell output via broadly responsive circuits with mitral and tufted relay neurons, enabling a wide odor responsiveness. In contrast, the connections that form between granule cells and mitral cells are sparser and more selective (Kato et al., 2013; Miyamichi et al., 2013). Surprisingly adult born interneurons also display characteristics distinct from early born interneurons, as adult neurogenesis generates granule cells more resistant to GABABR suppression of GABA release than granule cells born earlier in development (Valley et al., 2013). $Shh^{Ala/Ala}$ mice provide a valuable tool to identify distinctive roles for adult born calbindin-positive olfactory interneurons in olfactory signal transduction, and so may help explain why there is such extensive and persistent turn over in the adult olfactory system.

## Formation and Refinement of Glomerular Structures

Glomerular number appears to have important functional significance. Mutation of the potassium channel, Kv1.3, produces smaller, more numerous glomeruli

and is associated with heightened olfactory sensitivity and discrimination, producing "super-smeller" mice (Fadool et al., 2004). In contrast, deletion of the signaling component Adenylyl cyclase 3 (AC3) results in dramatically fewer glomeruli and greatly reduced olfactory sensitivity, while local overexpression of HCN4 channels reduces both the size and number of glomeruli in the olfactory bulb (Wong et al., 2000; Nakashima et al., 2013). In the future, large behavioral and electrophysiological studies will be needed to rigorously evaluate correlations between olfactory behavior and glomerular number in $Shh^{Ala/Ala}$ and other mutant mice with altered glomerular number.

The mechanisms that establish glomerular number and appropriate targeting are not yet understood. Glomerular development involves an initial phase during which individual glomerular structures coalesce, followed by a modification period in which aberrant connections are pruned. Initial glomerular formation takes place between E18.5 and P4 in mice (Royal and Key, 1999) and this corresponds to a critical period for establishing a functional olfactory map (Tsai and Barnea, 2014, Ma et al., 2014). In $Shh^{Ala/Ala}$ mice, Shh signaling within the bulb is not altered at this stage nor is early development of the olfactory bulb perturbed. Pruning of inappropriate OSN axons and elimination of aberrant innervation of multiple adjacent glomeruli normally occurs late in post-natal development. Consistent with this developmental program, in wild-type animals, the M71 and M72 glomeruli demonstrate heterogeneous OSN innervation at P10 but are homogeneously innervated by P60 (Zou et al., 2004). In $Shh^{Ala/Ala}$ mice, heterogeneous OSN innervation is observed at P10 and is retained in adulthood. Notably, the $Shh^{Ala/Ala}$ mice exhibit reduced Shh signaling in the olfactory bulb starting at P15, as ascertained by *Gli1* levels. This timeframe accords well with the stage at which the $Shh^{Ala/Ala}$ phenotype becomes evident (P15-P30) and with the stage at which glomerular pruning is reported to take place (Zou et al., 2004). The glomerular mixing defect in adult $Shh^{Ala/Ala}$ mice is therefore likely to reflect a role for Shh in glomerular refinement rather than a contribution to initial axon targeting of OSNs.

The process of glomerular pruning is partially dependent on sensory experience. Continuous post-natal olfactory sensory deprivation results in a failure to resolve “mature” M71 and M72 glomeruli (Zou et al., 2004). The data presented here suggest that Shh signaling that is initiated by Ptch1 and proteoglycan co-receptors may be a novel player in this later experience-dependent process of glomerular refinement. As OSNs express little, if any, of the known Shh receptors: Ptch1, Boc, Cdo or GPC5 (Gilad Barnea and Stavros Lomvardas, unpublished data), we postulate that Shh affects glomerular refinement via an indirect mechanism. As mitral cells both produce and respond to Shh, Shh might enhance segregation of dendrites emanating from distinct subpopulations of mitral cells. Thus Shh might alter expression of receptors such as neuropilins or CXCR4, which are expressed by mitral cells and have been implicated in glomerular innervation (Walz et al., 2002; Schwarting et al., 2004; Miyasaka et al., 2007). Periglomerular interneurons, whose proliferation is regulated by Shh, also express *Gli1* indicating that these cells have active Shh signaling during the postnatal period. Thus an alternative possibility is that reduced Shh signaling in inhibitory interneurons might alter excitatory-inhibitory balance in the olfactory bulb thereby affecting experience-dependent pruning.

Together these data indicate that the same signaling molecule act in different locations to achieve correct development of olfactory circuitry. In the SVZ, Shh regulates production of interneuron components that are integrated into the olfactory glomerular circuitry, while also acting within the olfactory bulb to determine glomerular parameters and innervation patterns. Thus Shh signaling regulates production of periglomerular interneurons and refinement of glomerular targeting in vertebrates. Similarly, in Drosophila, a coupled two-step mechanism coordinates the cell body position of OSNs and their glomerular targeting (Chou et al., 2010). Thus, a single signaling pathway coordinates spatially separate steps in establishment and maintenance of complex circuits in a manner conserved across evolution.

The authors thank Jennifer Kalscheuer and Emily Chadwick for help with mice. The authors thank Gilad Barnea for helpful discussion and for sharing unpublished results. Imaging was done at the Harvard NeuroDiscovery Center.

## REFERENCES

Akers KG, Sakaguchi M, Arruda-Carvalho M. 2010. Functional contribution of adult-generated olfactory bulb interneurons: odor discrimination versus odor memory. J Neurosci 30:4523–4525.

Alvarez-Buylla A, Garcia-Verdugo JM. 2002. Neurogenesis in adult subventricular zone. J Neurosci 22:629–634.

Angot E, Loulier K, Nguyen-Ba-Charvet KT, Gadeau AP, Ruat M, Traiffort E. 2008. Chemoattractive activity of sonic hedgehog in the adult subventricular zone

modulates the number of neural precursors reaching the olfactory bulb. Stem Cells 26:2311–2320.

Batista-Brito R, Close J, Machold R, Fishell G. 2008. The distinct temporal origins of olfactory bulb interneuron subtypes. J Neurosci 28:3966–3975.

Breton-Provencher V, Lemasson M, Peralta MR III, Saghatelyan A. 2009. Interneurons produced in adulthood are required for the normal functioning of the olfactory bulb network and for the execution of selected olfactory behaviors. J Neurosci 29:15245–15257.

Carleton A, Petreanu LT, Lansford R, Alvarez-Buylla A, Lledo PM. 2003. Becoming a new neuron in the adult olfactory bulb. Nat Neurosci 6:507–518.

Chan JA, Balasubramanian S, Witt RM, Nazemi KJ, Choi Y, Pazyra-Murphy MF, Walsh CO, et al. 2009. Proteoglycan interactions with Sonic Hedgehog specify mitogenic responses. Nat Neurosci 12:409–417.

Chou YH, Zheng X, Beachy PA, Luo L. 2010. Patterning axon targeting of olfactory receptor neurons by coupled hedgehog signaling at two distinct steps. Cell 142:954–966.

Fadool DA, Tucker K, Perkins R, Fasciani G, Thompson RN, Parsons AD, Overton JM, et al. 2004. Kv1.3 channel gene-targeted deletion produces "Super-Smeller Mice" with altered glomeruli, interacting scaffolding proteins, and biophysics. Neuron 41:389–404.

Fogarty M, Grist M, Gelman D, Marin O, Pachnis V, Kessaris N. 2007. Spatial genetic patterning of the embryonic neuroepithelium generates GABAergic interneuron diversity in the adult cortex. J Neurosci 27: 10935–10946.

Gong Q, Chen H, Farbman AI. 2009. Olfactory sensory axon growth and branching is influenced by sonic hedgehog. Dev Dyn 238:1768–1776.

Hor CH, Tang BL. 2010. Sonic hedgehog as a chemoattractant for adult NPCs. Cell Adh Migr 4:1–3.

Ihrie RA, Shah JK, Harwell CC, Levine JH, Guinto CD, Lezameta M, Kriegstein AR, et al. 2011. Persistent sonic hedgehog signaling in adult brain determines neural stem cell positional identity. Neuron 71:250–262.

Kato HK, Gillet SN, Peters AJ, Isaacson JS, Komiyama T. 2013. Parvalbumin-expressing interneurons linearly control olfactory bulb output. Neuron 80:1218–1231.

Lledo PM, Merkle FT, Alvarez-Buylla A. 2008. Origin and function of olfactory bulb interneuron diversity. Trends Neurosci 31:392–400.

Ma L, Wu Y, Qiu Q, Scheerer H, Moran A, Yu CR. 2014. A developmental switch of axon targeting in the continuously regenerating mouse olfactory system. Science 344: 194–197.

Miyamichi K, Shlomai-Fuchs Y, Shu M, Weissbourd BC, Luo L, Mizrahi A. 2013. Dissecting local circuits: parvalbumin interneurons underlie broad feedback control of olfactory bulb output. Neuron 80:1232–1245.

Miyasaka N, Knaut H, Yoshihara Y. 2007. Cxcl12/Cxcr4 chemokine signaling is required for placode assembly and sensory axon pathfinding in the zebrafish olfactory system. Development 134:2459–2468.

Mombaerts P. 2001. How smell develops. Nat Neurosci 4(Suppl):1192–1198.

Nakashima N, Ishii TM, Bessho Y, Kageyama R, Ohmori H. 2013. Hyperpolarisation-activated cyclic nucleotide-gated channels regulate the spontaneous firing rate of olfactory receptor neurons and affect glomerular formation in mice. J Physiol 591:1749–1769.

Palma V, Lim DA, Dahmane N, Sanchez P, Brionne TC, Herzberg CD, Gitton Y, et al. 2005. Sonic hedgehog controls stem cell behavior in the postnatal and adult brain. Development 132:335–344.

Potter SM, Zheng C, Koos DS, Feinstein P, Fraser SE, Mombaerts P. 2001. Structure and emergence of specific olfactory glomeruli in the mouse. J Neurosci 21:9713–9723.

Ressler KJ, Sullivan SL, Buck LB. 1994. A molecular dissection of spatial patterning in the olfactory system. Curr Opin Neurobiol 4:588–596.

Royal SJ, Key B. 1999. Development of P2 olfactory glomeruli in P2-internal ribosome entry site-tau-LacZ transgenic mice. J Neurosci 19:9856–9864.

Schwarting GA, Raitcheva D, Crandall JE, Burkhardt C, Puschel AW. 2004. Semaphorin 3A-mediated axon guidance regulates convergence and targeting of P2 odorant receptor axons. Eur J Neurosci 19:1800–1810.

Tsai L, Barnea G. 2014. A critical period defined by axon-targeting mechanisms in the murine olfactory bulb. Science 344:197–200.

Valley MT, Henderson LG, Inverso SA, Lledo PM. 2013. Adult neurogenesis produces neurons with unique GABAergic synapses in the olfactory bulb. J Neurosci 33:14660–14665.

Vassar R, Chao SK, Sitcheran R, Nunez JM, Vosshall LB, Axel R. 1994. Topographic organization of sensory projections to the olfactory bulb. Cell 79:981–991.

Walz A, Rodriguez I, Mombaerts P. 2002. Aberrant sensory innervation of the olfactory bulb in neuropilin-2 mutant mice. J Neurosci 22:4025–4035.

Witt RM, Hecht ML, Pazyra-Murphy MF, Cohen SM, Noti C, van Kuppevelt TH, Fuller M, et al. 2013. Heparan sulfate proteoglycans containing a glypican 5 core and 2-O-sulfo-iduronic acid function as Sonic Hedgehog co-receptors to promote proliferation. J Biol Chem 288: 26275–26288.

Wong ST, Trinh K, Hacker B, Chan GC, Lowe G, Gaggar A, Xia Z, et al. 2000. Disruption of the type III adenylyl cyclase gene leads to peripheral and behavioral anosmia in transgenic mice. Neuron 27:487–497.

Yu K, McGlynn S, Matise MP. 2013. Floor plate-derived sonic hedgehog regulates glial and ependymal cell fates in the developing spinal cord. Development 140:1594–1604.

Zhulyn O, Li D, Deimling S, Alizadeh Vakili N, Mo R, Puviindran V, et al. 2014. A switch from low to high shh activity regulates establishment of limb progenitors and signaling centers. Dev Cell 29:241–249.

Zou DJ, Feinstein P, Rivers AL, Mathews GA, Kim A, Greer CA, Mombaerts P, et al. 2004. Postnatal refinement of peripheral olfactory projections. Science 304:1976–1979.